Original Research Article

Spectroscopic and Kinetic Study of Sucrose Oxidation by Cr(VI) and its Application in the Quantitative Analysis of Soil Organic Carbon Content

.

ABSTRACT

The percent organic carbon (%OC) is an important soil fertility measure that has important implications in agricultural productivity and food security. In this study, a UV-visible spectrophotometric technique was investigated and applied to quantify %OC from selected soil samples along a river basin that traverses agricultural farmlands, a forest and sewage treatment lagoons for a comparative survey purposes. The study was based on the measurement of absorbance of Cr(III) species that arise from oxidation of sucrose (which is 42.11% carbon) by dichromate ions which contain Cr(VI) species. The uv-visible spectrophotometric double beam wavelength scan measurements elucidated the conversion of Cr(VI) to Cr(III) ions and a calibration plot was developed with r^2= 0.99. The analyte peak was identified in the region from 750 nm to 550 nm (the absorbing Cr(iii) species) with a turning point maximum at 576 nm. The kinetic profile of sucrose oxidation by the dichromate ions was studied via absorbance of Cr(III) and Cr(VI) as a function of the reaction time and was used to characterize the reaction model. The absorbance of Cr(III) as a function of reaction time fitted best into the non-linear Belehradek power function equation $y=a(x-b)^{c,}$, where y = absorbance; x = time(s); a, b, c = are constants (r^2 of 0.91). Kinetic analysis revealed that the reaction that leads to the formation of Cr(III) during sucrose oxidation proceeds via pseudo first-order kinetics (r^2= 0.83). A comparative quantitative analysis indicated that the sewage treatment lagoons had the highest %OC content at about 5.5-6.6 %OC. The soils sampled from the forest regions had about 4.6-5.8 % OC whereas the river bank soils had the lowest levels at about 2.0-2.5 %OC. A statistical *t*-test analysis showed that the %OC levels in sub-soils were significantly higher than those of the top-soils ($p > 0.05$ at 95% CI).

Keywords: UV-Vis Spectroscopy, Kinetics, Sucrose Oxidation, Organic Carbon, Chromium(VI)

1. INTRODUCTION

The ultraviolet-visible (UV-Vis) spectrophotometer has become one of the most widely used instrumental technique in many analytical and research laboratories. It has diverse applications such as in the monitoring of chemical or biochemical reactions and their kinetics, synthesis and characterization of organic and inorganic materials, quantitative analysis in pharmaceutical chemistry.[1-5] The UV-Vis spectroscopic technique measures how much ultraviolet or visible light a

certain molecule or chemical species absorbs in order to provide information that may be used to characterize its identity and/or its concentration. The technique is non-destructive, relatively simple in design, reliable and fairly low cost in terms of instrumentation for both coupled and direct methods.[6,7]

Soil organic carbon (SOC), the major and vital component of soil organic matter (SOM), consists of micro-organisms cells, plant and animal residues at various stages of decomposition, stable 'humus' synthesized from residues and nearly inert and highly carbonized compounds, such as charcoal, graphite and coal [8]. The SOM is crucial for the stabilization of soil structure, retention and release of plant nutrients and maintenance of water-retention capacity. This makes soil organic carbon a key indicator of not only soil health and its agricultural productivity but also its effect on the ecological functioning of ecosystems in the terrestrial environment.[9-12]

The percent organic carbon content (%OC) being an important parameter used in guiding decisions on choice of soil fertilizer application and irrigation in many plantations, its accurate determination has constantly and routinely been demanded from a many of soil-fertility testing laboratories. There has been some interest among chemists in the investigation and optimization of methods and techniques for the accurate quantification or estimation of %OC content in soils samples.[13-15] In this study, a modified UV-Vis spectrophotometric for the determination of %OC based on the conversion of Cr(VI) to Cr(III) by sucrose standards is investigated spectroscopically. The kinetics of the sucrose oxidation reaction is also presented including the effects of reaction time and temperature on it. Finally, a comparative analysis of the quantification of %OC levels is made based on measurements from the soil samples extracted from selected zones around river Njoro basin catchment area, Egerton, Nakuru, Kenya.

2. MATERIAL AND METHODS

2.1 Preparation of Standard Solutions and the Oxidizing Reagent

A stock solution of 1000 ppm was prepared by measuring 0.5 g of sucrose into a 500 ml volumetric flask and topping to the mark using double distilled water. Aliquots of 0.5, 2.5, 4.0, 7.5, 10.0, 12.5, 15.0, 17.5, 20.0, 22.5, 35.0, and 40.0 ml of the sucrose stock solution were each withdrawn using a pipette and released into individual 50 ml volumetric flasks. A 1N $K_2Cr_2O_7$ solution was prepared by weighing exactly 7.35 g of $K_2Cr_2O_7$ using an analytical balance and adding 50 ml of distilled water to it in a measuring cylinder. A solution of 1ml of 1N $K_2Cr_2O_7$ and 2 ml of H_2SO_4 acid was prepared as the working oxidizing reagent that was added onto each of the standard solutions.

2.2 Preparation of Soil Samples for UV-VIS Spectrophotometric Analysis

The sampled soils were crushed and air-dried on aluminum foil for one week. The soil samples were sieved using a 2 mm sieve. The sieved samples were then put in a mortar and ground using a pestle to a fine texture after which 1 g of the various samples were measured and placed into separate 50 ml volumetric flasks containing 1ml of 1N $K_2Cr_2O_7$ oxidizing agent and 2 ml of 18M H_2SO_4 acid. The mixtures were allowed to stand for about 10 minutes and were then each topped to the mark using distilled water. The mixtures were then heated at 40 ℃ for about 10 minutes and then left to stand for four weeks. The absorbance values for each of the samples were then measured using the UV–Visible spectrophotometer at 576 nm and recorded. The calibration plots developed for %OC determination were then used to determine the %OC levels for the soil samples.

3. RESULTS AND DISCUSSION

3.1 Basis of the spectrophotometric experiment

The reaction is based on the conversion of Cr(VI) to Cr(III) ions which happens during the oxidation of sucrose in acidified potassium dichromate solution. The absorption of Cr(III) species which are formed during the oxidation is sucrose reaction is measured using spectrophotometer. Its amount is proportional to the sucrose concentration (and hence used to estimate %OC content in the sample since sucrose is about 42.1% Carbon) based on the Beer-Lambert relation. The absorbance of Cr(III) as a function of time can also be used to investigate the kinetics of the chemical reaction. Figure 1 shows the electronic absorption spectra derived from wavelength scan measurements of the oxidizing reagent (in black), sucrose solution (in red) and a spectrum of the product after a given time interval (in blue). The oxidizing reagent and the sucrose solution are the principal reactants and are indicated in the chart to serve as reference spectra.

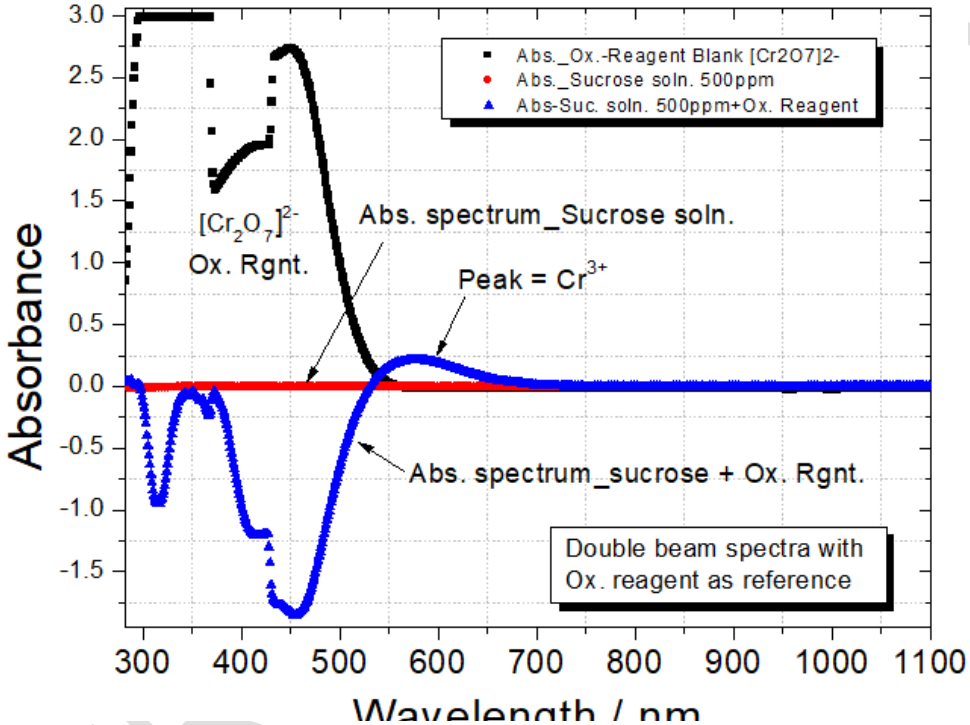

Fig. 1: Electronic Absorption Spectrum of Oxidizing Reagent (reference blank), Sucrose Solution (reference blank) and Sucrose Solution (Treated with the Oxidizing Agent)

The absorption band observed in the blue spectrum within the range from about 700 nm to 570 nm confirms the presence of Cr(III) ions as a product arising from sucrose oxidation by the dichromate solution. This is the analyte peak and the absorption band is absent in both the red and blue reference spectra. The Cr(III) ions are known to exhibit an absorption band in the visible region with a lambda maximum value of about 550 nm.[16] Its actual absorption band is partially masked by the absorption band of Cr(VI) that begins at about 570 nm within neighboring range. The spectrum obtained from sucrose solution (depicted in red) is UV-Vis inactive as it shows no absorption band between 1100 – 300 nm. In the absorption spectrum of the sucrose + oxidizing agent (depicted in blue) the bands in the range between about 550 – 300 nm that appear pointing downwards (and somehow symmetrical to those of the oxidizing reagent within the same range) are due to the subtracted absorption values related to the oxidizing agent (dichromate) as reference. This is because the measurements are conducted in a double beam manner in which the oxidizing agent is fixed the reference while the sucrose + oxidizing reagent solution is fixed as the main sample in the spectrophotometer.

3.2 Elucidation of the analyte peak resulting from Cr(III) absorption in the standard solutions

Figure 2 shows wavelength scan measurements obtained from a series of the standard solutions as well as the reference spectra of the reactants. An analyte peaks appears between 550-700 nm with the turning point at 576 nm for all the sucrose solutions treated with the oxidizing reagent. The analyte peak is related to appearance of Cr(III) and is sensitive to the concentrations of sucrose standards. It can be observed that the analyte peak responds to concentration of the substrate. This is because greater peak area and heights are recorded for higher sucrose concentrations treated with the dichromate ions. Sucrose solution of 5 ppm in concentration treated with the oxidizing reagent however shows no appreciable absorbance for Cr(III) ions.

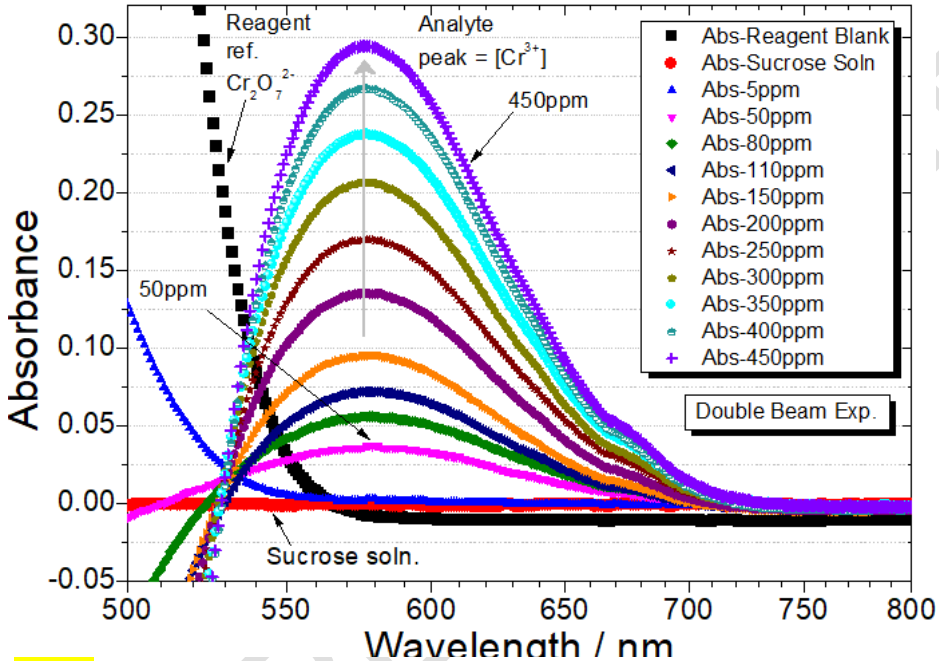

Fig. 2: Absorbance spectra of the analyte peak of the standards

This provides clear illustration that the Cr(VI) in the dichromate $Cr_2O_7^{2-}$ ions converts to give Cr(III) upon interacting with sucrose in acidified solution. The higher the concentration of sucrose substrate, the higher the Cr(III) analyte peak. The analyte peak is appearing asymmetrical due to the subtraction of absorbance values of the oxidizing reagent, which was used as the reference during double beam experiment. Analyte peak heights at 576 nm obeys the beer Lambert law within the concentration range of the standards used in the investigation as the absorbance is proportional to the concentration of the substrate.

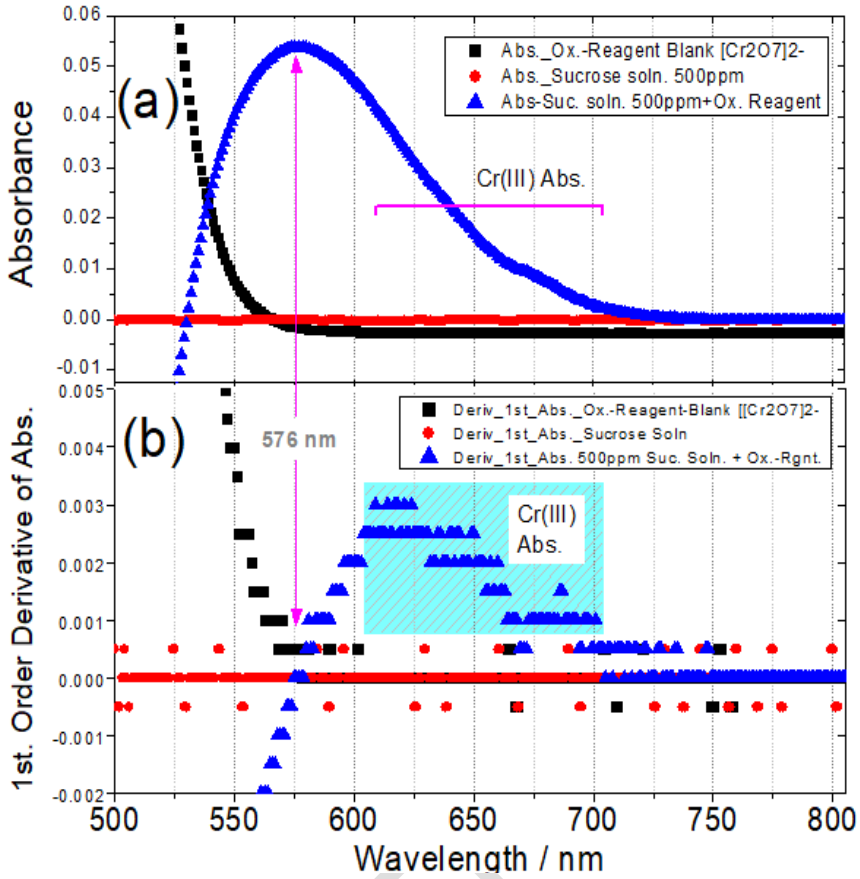

Fig. 3: (a) Absorbance vs. wavelength and (b) The first - order derivative graph

Figure 3 shows overlay graph from spectroscopic data extracted from Figure 2 (labeled as (3a)) and the first order derivative graph of the same (labelled as 3b). The purpose of derivatization is to give more detailed characterization of the Cr(III) absorption band. It confirms that the analyte peak (related to Cr^{3+}) begins to rise from about 750 nm towards 576 nm. It also has shoulder peak at about 690 nm (Fig. 3b), this extra piece of information further characterizes the absorption band of the Cr(III) species in the solution and is consistent with previous findings [17].

3.3 Dependence of the Cr(III) analyte peak on reaction time and substrate concentration

Figure 4 highlights the absorption spectra obtained from a series of wavelength scan measurements aimed at characterizing the dependence of sucrose oxidation on the substrate concentration and reaction time. The four graphs in Figure 4 depict the behavioral trend of the analyte peak over time for selected substrate concentrations. The reactions were monitored from day one up to 5 days (or 120 hrs.) for different concentrations. In Figure 4 (a), at 300 ppm sucrose solution treated with the oxidizing reagent, the analyte peak rises shows appreciable formation of Cr(III) from about 1hr (spectrum in brown). There is a large gap in peak height between the first hour and the 24th hour from the onset of the reaction.

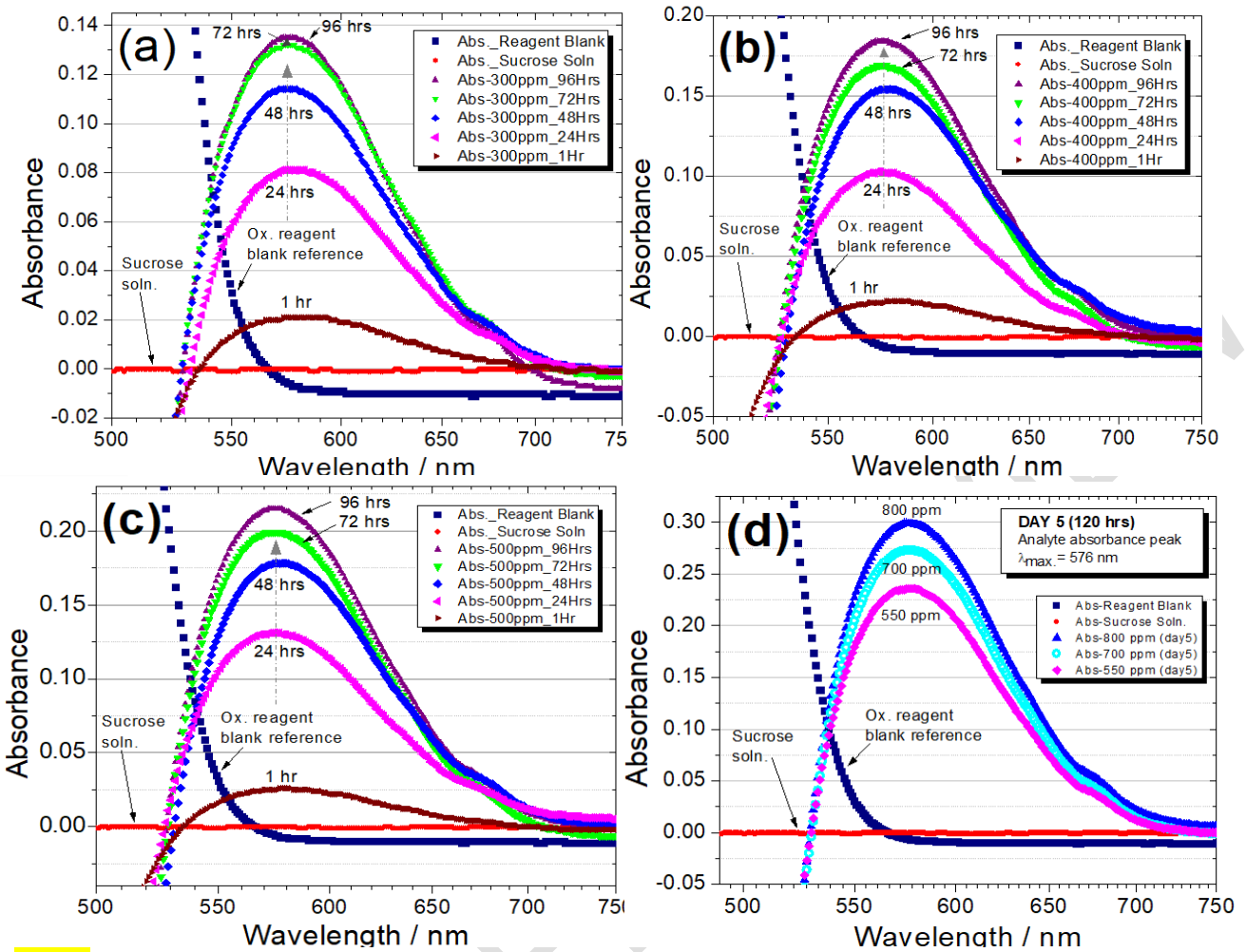

Fig. 4: Dependence of the Cr(III) analyte peak on reaction time and the sucrose substrate concentration

A smaller gap in peak height is observed between the 24th and 48th hour. The hours which extend into days (Figures 4a, b and c) also display some gradual increase in Cr(III) absorption with marginal differences between 72 and 96 hours in all the three cases. This means that the reaction that leads to the formation of Cr(III) occurs mush faster within the first 48 hrs. and rate diminishes from about day 3 (72 hours) onwards.

In Figure 4(d), which depicts the 5 day (120 hrs.) experiment, relatively higher absorbance values are obtained for a set of 550, 700 and 800 ppm sucrose solutions treated with the oxidizing agent. Also the analyte peak is responsive to the concentration of sucrose substrate as the 800 ppm has greater peak height and area than that of 700 ppm, while the 500 ppm peak has the lowest value of the three. This trend as depicted by experiments in Figure 4 characterizes the oxidation of sucrose solution with potassium dichromate in the presence of an acid as a reaction that is fairly faster within the first 48hrs but can still accumulate its products over a couple of days later at slower rate.

3.4 Stability of the dichromate oxidizing agent and effect of addition of 18M H_2SO_4 on its Absorption band

Figure 5 shows the wavelength scan measurements for the acidified dichromate oxidizing solution when exposed to natural light at room temperatures taken over time to check on its stability. The 3-D wave plot profile for stability of the oxidizing agent over time shows no significant variation in the

absorption bands with maximum absorption at 450 nm. This means that the identity and composition of the acidified dichromate ions does not change when stored in even in transparent reagent bottles.

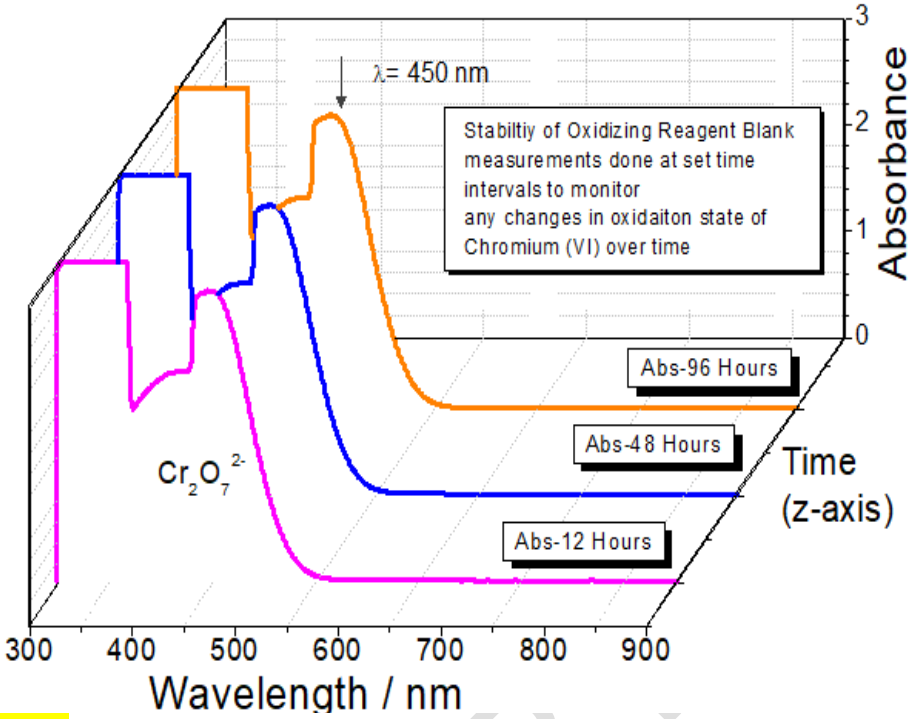

Fig. 5: Absorption spectra of the dichromate ion solution over time

Figure 6 depicts the absorption bands of the dichromate oxidizing reagent in aqueous phase only (in blue) versus when 18M H_2SO_4 acid is added to it (in red). It can be observed that the addition of 18M H_2SO_4 acid has no significant change on the absorption band except that it creates band broadening. The extensive hydrogen bonding interactions resulting from the introduction of hydrogen ions and increased disorder or entropy due to effect of sulphate interference are possible contributing factors to the band broadening. Band broadening phenomenon has been observed in a number spectroscopic investigations and have been attributed to changes in nature of solvents, and increased hydrogen bonding interactions.

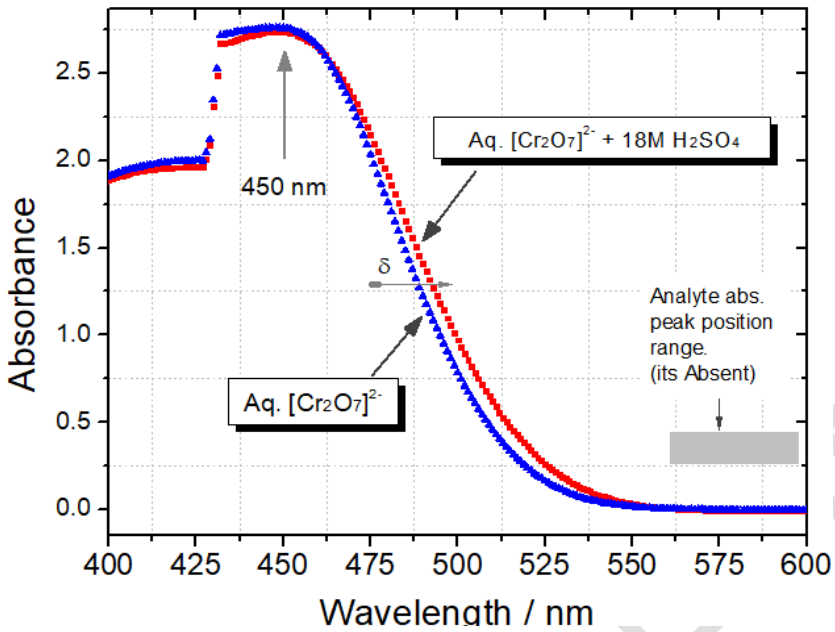

Fig. 6: Broadening of the dichromate ion absorption band due to addition of 18M H_2SO_4 acid

It can also be observed in Figure 6 that both spectra possess no absorption bands around 600 – 550 nm, which is the typical region for the Cr(III) absorption band as elucidated earlier in Figures 1 and 2. This shows that addition of acid has no effect on the emergence of the Cr(III) analyte peak except when sucrose solution react with it leading to the conversion of the Cr(VI) ions to Cr(III) ions.

3.5 Evaluation of the kinetic profile of sucrose oxidation

Figure 7 is a graphical representation of the absorption of Cr(III) ions during the course of the sucrose oxidation reaction with dichromate ions monitored at wavelength of 576 nm within the first 10,000 seconds at room temperature. A rise in the concentration of the Cr(III) (a product) is observed over time from the kinetic investigation. The absorbance versus time data best fits into a power function of the form $y=a(x-b)^c$ with $R^2 = 0.91$. It can be observed that the absorbance of Cr(III) tends to stay constant over brief periods before the increments happen in a step-wise fashion to higher absorbance values.

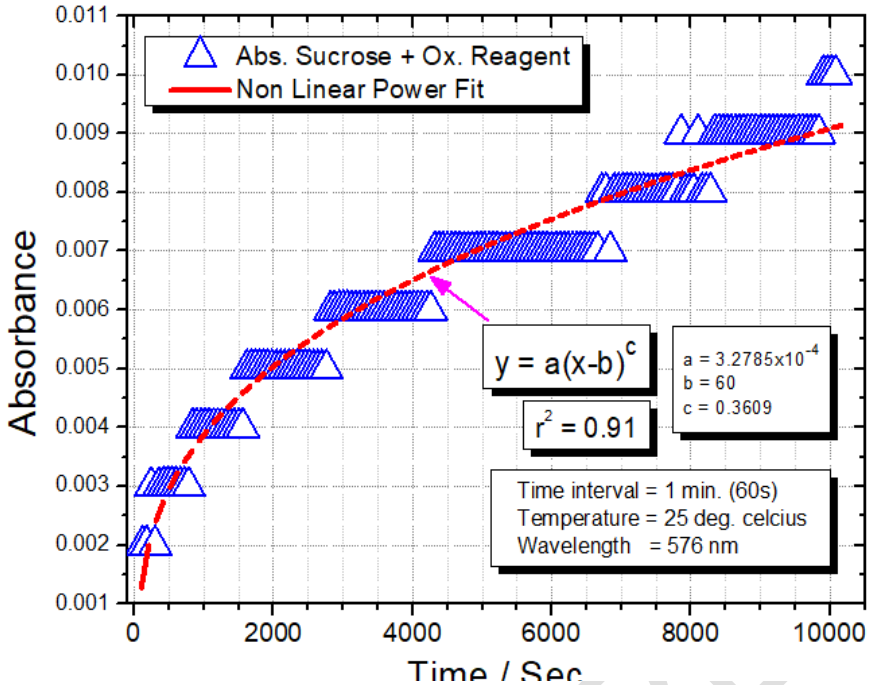

Fig. 7: Graph of absorbance of Cr(III) at 576 nm as a function of reaction time

The step-wise pattern is observed throughout the experiment. The absorbance readings of Cr(III) tends to stay static over longer time periods as the reaction progresses to later stages as opposed to earlier stages. It can be assumed that the rate of appearance of Cr(III) species mimics the rate of formation of sucrose oxidation products in the course of the reaction. The pattern characterizes the reaction of a typical bulky substrate (such as sucrose in this case) that tends to favor unimolecular mechanism, where the rate determining step is the slowest one.

3.5.1 Graphical fitted test for first- and second- order kinetics

The kinetic experiments are based on the premise that the recorded absorbance values of Cr(III) species follow the rate of formation of the oxidation products of sucrose as the reaction proceeds. Information about the order of the reaction can be derived from graphical analysis using fitted tests as discussed herein. Zero order kinetics is ruled out from the fitted absorbance versus time graph in Figure 7, where the data fits best into an exponential curve rather than a linear fit.

Figure 8(a) shows the fitted test for first order kinetics based on the absorbance values of the Cr(III) product which is formed during the oxidation of sucrose reaction in kinetic photometric experiment carried out for 10,500 seconds. The plot is based on the integrated law for first order kinetics where ln(Abs.) is plotted as function of time.

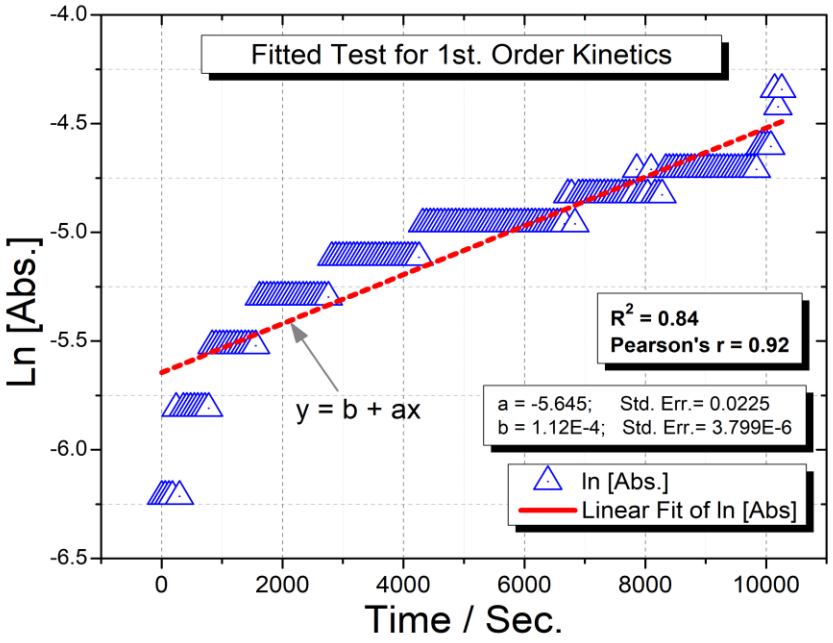

Fig. 8(a): Fitted test for First - Order Kinetics

A linear fit of the data gives an R. square value of 0.83 and Pearson's correlation coefficient of +0.91. The equation of the regressed line of best fit is y = -5.645 + 0.000112(x). The standard errors in the intercept and slope as tabulated in the Figure 8a are 0.0225 and 3.799 x 10^{-6} respectively.

Fig. 8b shows the fitted test for second-order kinetics based on the absorbance values of the Cr(III) product which is formed during the oxidation of sucrose reaction in kinetic photometric experiment carried out for 10,500 seconds. The plot is based on the integrated law for second- order kinetics where the inverse values of absorbance is plotted as function of time.

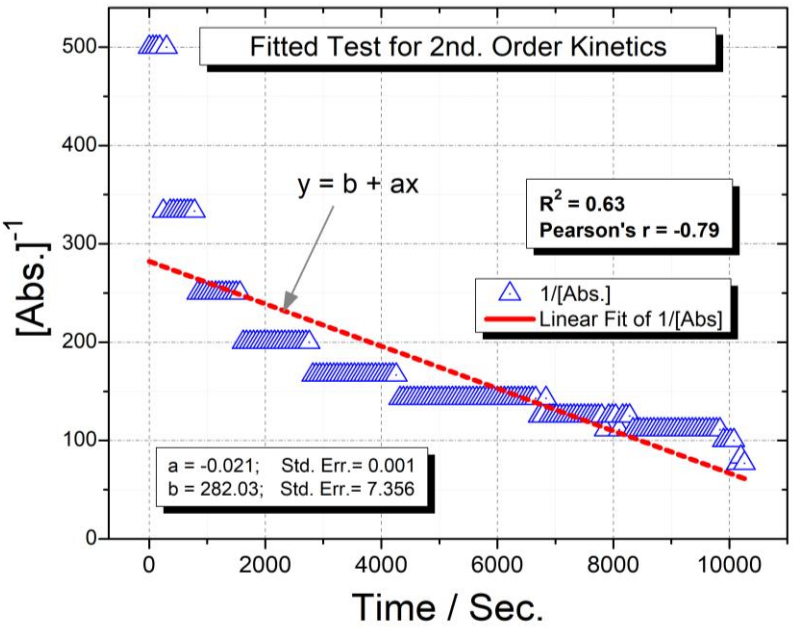

Fig. 8(b): Fitted Test for Second - Order Kinetics

A linear fit of the data into the second-order linear equation gives an R- square value of 0.63 and Pearson's correlation coefficient of -0.79 under the conditions of investigation. The equation of the

regressed line of best fit is y = -0.021 + 0.282(x). The standard errors in the intercept and slope as tabulated in Figure 8b are 0.001 and 7.356 respectively.

The R- square value for the fitted test for first-order kinetics is higher (0.91) than that of the fitted test for second-order kinetics (0.63). It can also be noted that the standard errors in the slope and intercept in the fitted test for second-order kinetics are of greater magnitudes than in the fitted test for first order kinetics. This means that the absorbance values recorded for Cr(III) versus time data fits better in first-order kinetics as opposed to second-order kinetics. Considering that water is abundant in the system and the concentration of the oxidizing Cr(VI) is in excess, it can be concluded that the oxidation of sucrose under such experimental conditions proceeds via pseudo-first order kinetics [18].

3.5.2 Reaction modelling based on Cr(VI) and Cr(III) species and effect of temperature

Figure 9(a) shows a graph that models the kinetic profile of the conversion of Cr(VI) to Cr(III) ions during sucrose oxidation. The absorption of Cr(VI) (a reactant) was measured at 450 nm, while that of Cr(III) (a product) was measured at 550 nm. The kinetic experiments conducted separately under similar conditions in photometric mode are represented in Figure 9a, in which the reaction vessel was initially heated to 40 ^{o}C for each case. The spectrum in red shows how the concentration of Cr(VI) ions are decreasing while that of Cr(III) in blue is increasing over the first 2000 seconds. The graph model the conversion of Cr(VI) to Cr(III) during sucrose oxidation by the oxidizing dichromate ions. Under the experimental conditions, it can be noted that the rate of change in the product formation seems to occur much faster initially within the first 500 s as opposed to the later stages of the reaction. This characterizes the effect of heat which is initially applied to the reaction meaning that the reaction is temperature dependent.

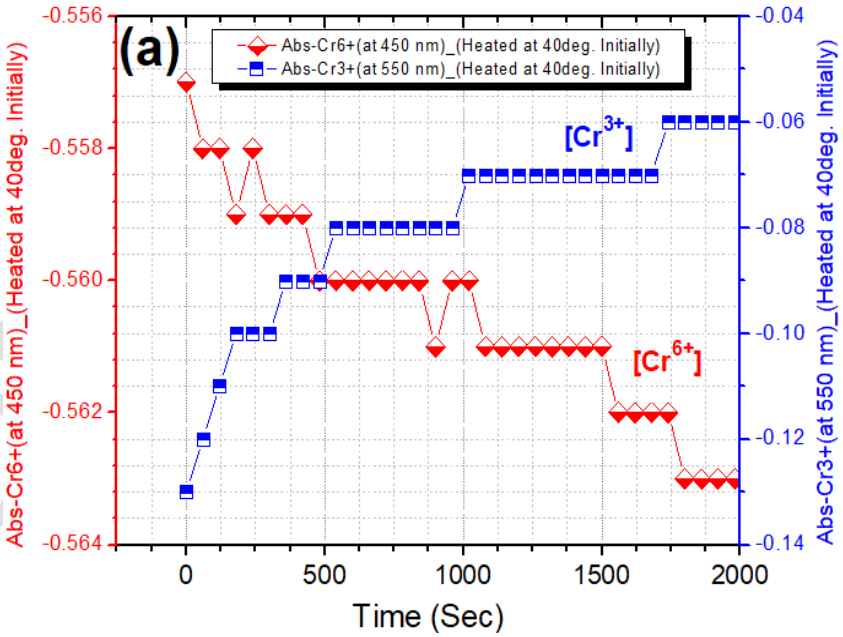

Fig. 9(a): Kinetic profile that represents the conversion of Cr(VI) reactant to Cr(III) product under heated conditions

Figure 9(b) shows the kinetic profile of the Cr(VI) reactant and Cr(III) product absorbance data recorded during sucrose oxidation at room temperature conditions (or unheated) for the first 2000 s. It can be observed from the Figure 9(b) that absorbance values of Cr(III) tends to stay constant or static over longer periods in the unheated reaction case when compared to the case in which the reaction is initially warmed/heated to 40 ^{o}C (Figure 9a).

In Figure 9(b), (the unheated case) it can also be noted that the rate of decrease in concentration of the reactant Cr(VI) seems to occur faster than the rate of increase in concentration of the Cr(III) product within the first 500 s. This possibly indicates the formation of other oxidation states of Cr other than the measured Cr(III) species.

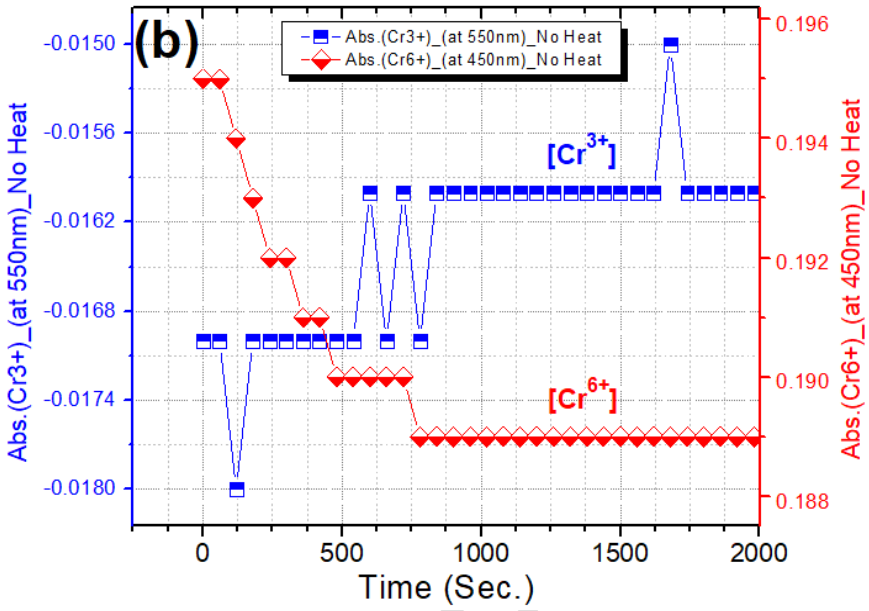

Fig. 9(b): Kinetic profile of the Cr(VI) reactant and Cr(III) product absorbance data recorded during sucrose oxidation under room temperature conditions for the first 2000 s

The observed periodic rise and fall in absorbance values as depicted in the Cr(III) curve (Figure 9b) and Cr(VI) curve (Figure 9a) are most likely an indication of side reactions that play role in sequestering the metal ions in solution hence partially blocking it from its interaction with the light path for the absorbance measurements. Such interfering reactions may possibly involve metal chelation mechanisms when the sucrose molecules in solution behave as the metal chelating agents.

4.0 Determination of the %OC in Soil Samples and a Comparative Analysis

4.1 Calibration plot for the determination of the %OC

Figure 10 below shows the graph of calibration plot derived from absorbance measurement of the standards solutions of sucrose. The absorbance measurements were obtained from photometric measurements at 576 nm, where the double beam experiment depicts greatest response to analyte concentration as discussed in the earlier in Figure 2. The plot of absorbance versus concentration of the sucrose standards shows linear dependence with and R square value of 0.99 and therefore obeys the Beer-Lambert equation.

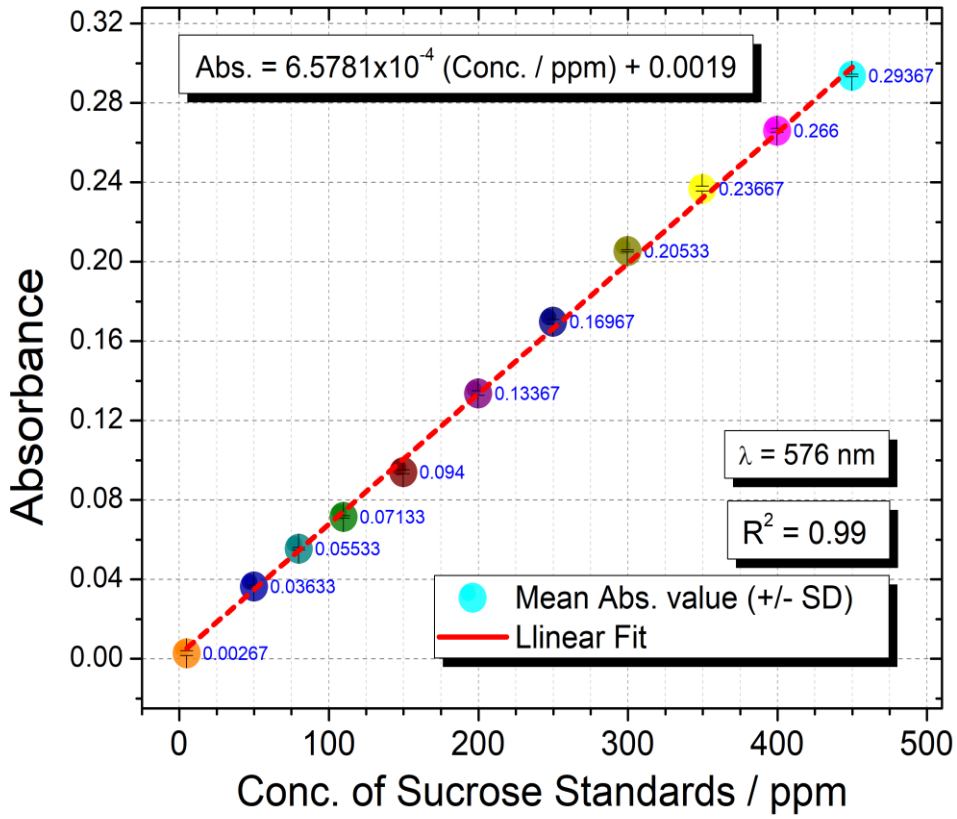

Fig. 10: Calibration plot for carbon content estimation based on Cr(III) absorbance values

A scrutiny of the curve shows that the absorbance values increase by similar factor as the increments in concentrations of sucrose standards. For example, when the concentration of sucrose doubles from 100 ppm to 200 ppm, the measured absorbance value of Cr(III) product increases by a factor of two. Similarly, when the concentration triples from 100 ppm to 300 ppm, the absorbance value also triples. This behavior mimics the classical characteristic of first-order kinetics. Because the oxidizing reagent is present in excess and the concentration water in unity, the analysis lends credence to earlier conclusion that the reaction proceeds via pseudo-first order kinetics.

Figure 11 shows the standard conversion chart for the determination of %OC based on the calibration plot developed from the sucrose standards depicted in the earlier Figure 10. The standard conversion chart is based on the fact that sucrose is 42% carbon in terms of elemental composition, such that a 100 ppm sucrose solution represents approximately 0.4211 % OC. A sucrose solution of 200 ppm would represent 0.84 %OC and so and so forth.

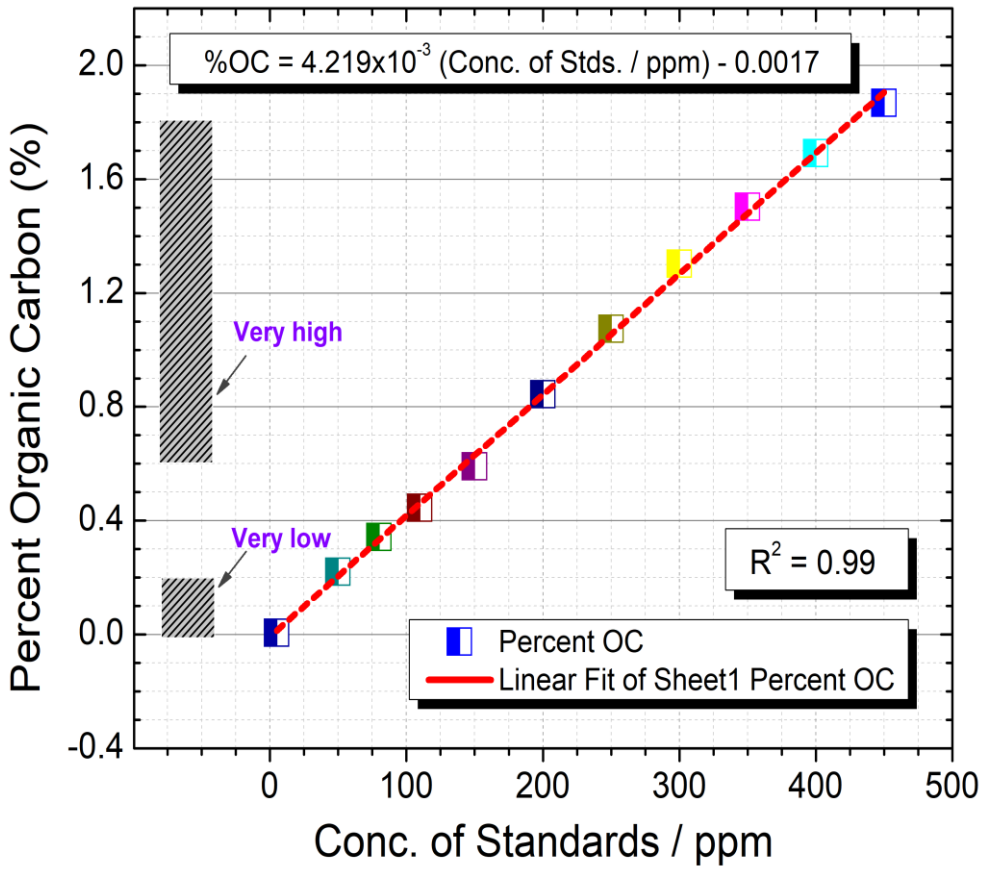

Fig. 11: Conversion chart for the estimation of %OC in soil samples

It is the absorbance measurement values from the soil samples that provide the estimated sucrose concentrations (Figure 10), which are then converted to %OC levels. The equation for the standard conversion curve is %OC = 0.0042 (Sucrose conc. in ppm) - 0.1111. As indicated in the chart, %OC values greater than 0.6 are generally considered very high while %OC values of less than 0.2 are considered very low.[19] Very high levels of %OC generally predict high levels of soil organic matter (SOM) in the particular environment from which the sampling is done.

4.2 Comparative analysis of the %OC values of the selected zones

The estimation of %OC is based on equation 1 from the spectrophotometric measurements derived from Figures 10 and 11. The equation permits a fast computation of the %OC from the absorbance values measured by photometric means at a fixed wavelength of 576 nm from the prepared soil samples.

$$\%\mathrm{OC} = 0.0042\left(\frac{Mean\ Abs._{@576\ nm} - 0.0019}{6.5781\ x\ 10^{-4}}\right) - 0.0017 \qquad \text{Eqn. ------- 1}$$

Figure 12 shows a histogram chart that compares the percent OC obtained from upper, mid-, and lower lagoons in the sewage treatment plant near the banks of River Njoro downstream. The computed % OC levels from the three sampling sites depict generally high %OC since all the resulting computed average values are higher than 0.6%. The %OC recorded from the soil samples of the sewage treatments plant lagoons was found to be significantly higher than those obtained from the other sampling sites

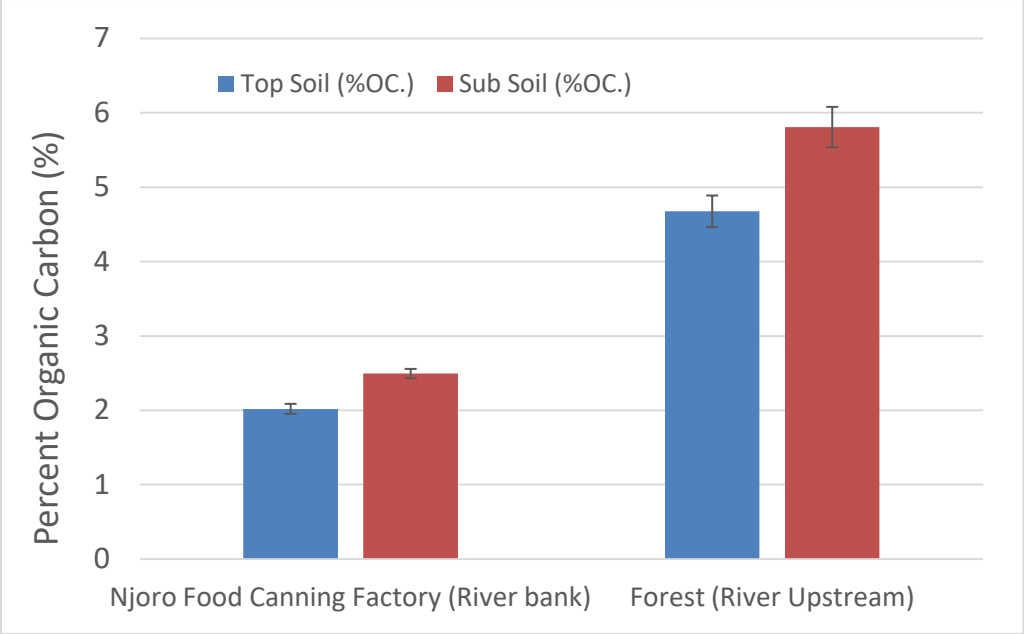

Fig. 12: %OC levels of River bank next to Njoro food canning factory and Nessuiet Forest

.

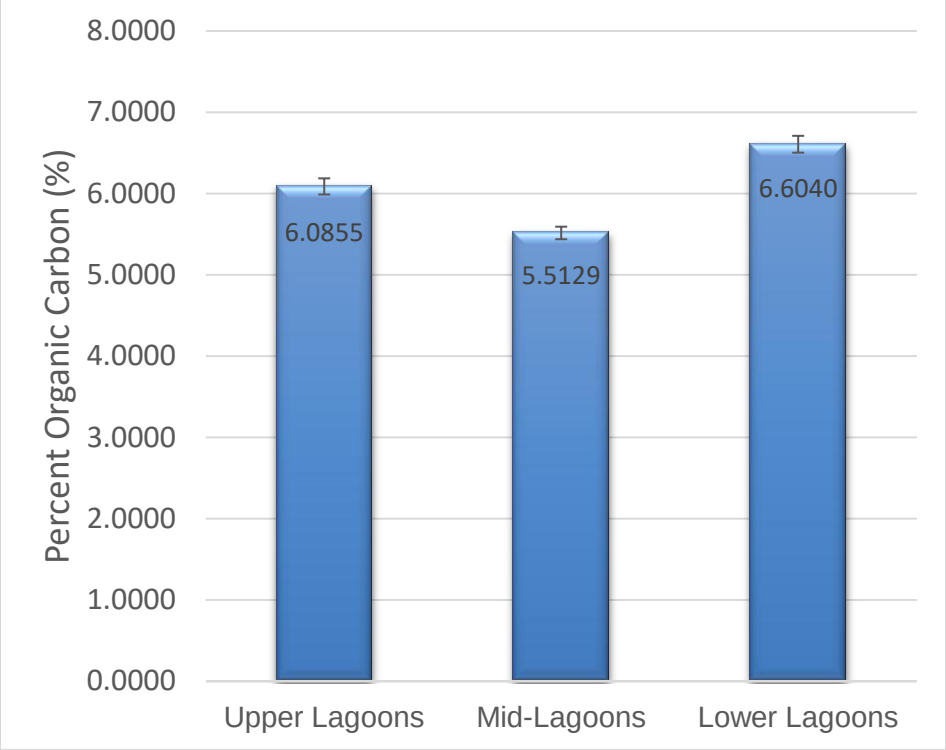

Fig.13: Histogram chart comparing the percent OC obtained from upper, mid-, and lower sewage treatment plant lagoons near the banks of River Njoro

The main factor that could explain this result is the existence of the sewage drainage infrastructure continually introducing the disposed organic refuse into the lagoons, which in the long term, leads to the accumulation of extra organic matter in the soils. The disposed matter includes materials ranging from food-stuff residues, fecal discharge, and even the used waters containing soaps and detergents.

The main factor that could explain this result is the existence of the sewage drainage infrastructure continually introducing the disposed organic refuse into the lagoons, which in the long term, leads to the accumulation of extra organic matter in the soils. The disposed matter includes materials ranging from food-stuff residues, fecal discharge, and even the used waters containing soaps and detergents.

4. CONCLUSION

The kinetic and spectroscopic investigations of a UV-Visible spectrophotometric technique based on the conversion of Cr(VI) to Cr(III) ions resulting from the oxidation of sucrose by the dichromate ions ($Cr_2O_7^{2-}$) in an acidic medium was conducted successfully to characterize the reactions. The spectroscopic experiments elucidated the analyte peak in the region from 750 nm to 550 nm (indicating the presence of the absorbing Cr(III) species). The UV-Visible spectrophotometric double beam wavelength scan measurements characterized the conversion of Cr(VI) to Cr(III) ions during the sucrose oxidation process. The measured absorbance of the Cr(III) species (producing the analyte peak that forms during the oxidation process) was found to be related to the initial substrate (sucrose) concentration and therefore obeyed the Beer-Lambert equation. The calibration plot equation developed was used to quantify the %OC levels from selected soil samples.

The graphical fitted tests of the kinetic profile of sucrose oxidation based on the integrated rate law models using the photometric measurements revealed that the rate of formation of sucrose oxidation product(s) under the conditions of the investigation proceeds via pseudo-first-order kinetics (R^2 = 0.91). The rate constant for the reaction was determined to be 3.799×10^{-6} s^{-1}. Further, photometric kinetic measurements were successfully used to depict the reaction model for the sucrose oxidation reaction based on the conversion of Cr(VI) (as reactant) to Cr(III) (as product). The effect of heat on the sucrose oxidation reaction was also modeled to determine temperature dependence, which showed that initial heating of the reaction enhances the rate of the reaction substantially.

The photometric analysis showed that all the regions investigated had very high %OC levels. The %OC levels were highest in the sewage treatment lagoons. The levels of %OC in the forest (river bank upstream) were found to be significantly higher than those obtained from the R. Njoro bank (downstream) next to Njoro Canning Factory. A paired 2- tailed independent *t*-test analysis showed that there is no significant difference in %OC values between the top-soil and sub-soil samples (p_{value}<0.05 at 95% CI).

DISCLAIMER:

Authors have declared that no competing interests exist. The products used for this research are commonly and predominantly used products in our area of research and country. There is absolutely no conflict of interest between the authors and producers of the products because we do not intend to use these products as an avenue for any litigation but for the advancement of knowledge. Also, the research was not funded by the producing company rather it was funded by personal efforts of the authors.

REFERENCES

(1) Andris, S.; Rüdt, M.; Rogalla, J.; Wendeler, M.; Hubbuch, J. Monitoring of Antibody-Drug

Conjugation Reactions with UV/Vis Spectroscopy. *J. Biotechnol.* **2018**, *288*, 15–22.
(2) Lauterbach, F.; Abetz, V. Continuous Kinetic Sampling of Flow Polymerizations via Inline UV–Vis Spectroscopy. *Macromol. Rapid Commun.* **2020**, *41* (9), 2000029.
(3) Begum, R.; Farooqi, Z. H.; Naseem, K.; Ali, F. Applications of UV / Vis Spectroscopy in Characterization and Catalytic Activity of Noble Metal Nanoparticles Fabricated in Responsive Polymer Microgels : A Review. *Crit. Reviwes Anal. Chem.* **2018**, *48* (6), 503–516.
(4) Ben Salah, M.; Aouadhi, C.; Khadhri, A. Green Roccella Phycopsis Ach. Mediated Silver Nanoparticles: Synthesis, Characterization, Phenolic Content, Antioxidant, Antibacterial and Anti-Acetylcholinesterase Capacities. *Bioprocess Biosyst. Eng.* **2021**, *44* (11), 2257–2268.
(5) Angheluta, A.; Guizani, S.; Saunier, J.; Rönnback, R. Application of Chemometric Modelling to UV-Vis Spectroscopy: Development of Simultaneous API and Critical Excipient Assay in a Liquid Solution Continuous Flow. *Pharm. Dev. Technol.* **2020**, *25* (8), 919–929.
(6) Perkampus, H.-H. *UV–VIS Spectroscopy*, 1st ed.; H. Charlotte Grinter and Dr. T. L. Threlfall, Ed.; Springer -Verlag: Berlin, 1992.
(7) Pluczyk, S.; Vasylieva, M.; Data, P. Using Cyclic Voltammetry, UV-Vis-NIR, and EPR Spectroelectrochemistry to Analyze Organic Compounds. *J. Vis. Exp.* **2018**, *140*, 56656.
(8) Blanco-Canqui, H.; Shapiro, C. A.; Wortmann, C. S.; Drijber, R. A.; Mamo, M.; Shaver, T. M.; Ferguson, R. B. Soil Organic Carbon: The Value to Soil Properties. *J. Soil Water Conserv.* **2013**, *68* (5), 2–3.
(9) Obalum, S. E.; Chibuike, G. U.; Peth, S.; Ouyang, Y. Soil Organic Matter as Sole Indicator of Soil Degradation. *Environ. Monit. Assess.* **2017**, *189* (4), 176.
(10) Ondrasek, G.; Bakić Begić, H.; Zovko, M.; Filipović, L.; Meriño-Gergichevich, C.; Savić, R.; Rengel, Z. Biogeochemistry of Soil Organic Matter in Agroecosystems & Environmental Implications. *Sci. Total Environ.* **2019**, *658*, 1559–1573.
(11) Baveye, P. C.; Schnee, L. S.; Boivin, P.; Laba, M.; Radulovich, R. Soil Organic Matter Research and Climate Change: Merely Re-Storing Carbon Versus Restoring Soil Functions. *Front. Environ. Sci.* **2020**, *8* (September), 1–8.
(12) Van Meter, R. J.; Glinski, D. A.; Henderson, W. M.; Purucker, S. T. Soil Organic Matter Content Effects on Dermal Pesticide Bioconcentration in American Toads (Bufo Americanus). *Environ. Toxicol. Chem.* **2016**, *35* (11), 2734–2741.
(13) De Souza, D. M.; Morais, P. A. de O.; Matsushige, I.; Rosa, L. A. Development of Alternative Methods for Determining Soil Organic Matter. *Rev. Bras. Cienc. do Solo* **2016**, *40*, 1–17.
(14) Escalona, Y.; Petrov, D.; Oostenbrink, C. Vienna Soil Organic Matter Modeler 2 (VSOMM2). *J. Mol. Graph. Model.* **2021**, *103*, 107817.
(15) Jollymore, A.; Johnson, M. S.; Hawthorne, I. Submersible UV-Vis Spectroscopy for Quantifying Streamwater Organic Carbon Dynamics: Implementation and Challenges before and after Forest Harvest in a Headwater Stream. *Sensors* **2012**, *12* (4), 3798–3813. https://doi.org/10.3390/s120403798.
(16) Hamada, Y. Z.; Bayakly, N.; Shafi, M.; Painter, S.; Taylor, V.; Greene, J.; Rosli, K. Reactions of Cr(3+) with Aspartic Acid within a Wide PH Range. *Complex Met.* **2014**, *1* (1), 46–51.
(17) Soares, R.; Carneiro, M. C.; Monteiroa, M. I. C.; Henriquae, S. de S.; Pontes, F. V. M.; Dias da Silva, L. I.; Neto, A. A.; Santelli, R. E. Simultaneous Speciation of Chromium by Spectrophotometry and Multicomponent Analysis. *Chem. Speciat. Bioavailab.* **2009**, *21* (3), 153–160.
(18) Scientist, F. Florida Academy of Sciences , Inc . Reaction of chromium (VI) wastes with sugars Author (s): Chuhua Wang , Dean F . Martin and Barbara B . Martin Published by : Florida Academy of Sciences , Inc . Stable URL : Https://Www.Jstor.Org/Stable/24320961. **2021**, *62* (1), 48–57.
(19) Ravikumar, P.; Somashekar, R. K. Evaluation of Nutrient Index Using Organic Carbon, Available P and Available K Concentrations as a Measure of Soil Fertility in Varahi River Basin ,

India. **2013**, *3* (4), 330–343.